Original paper

Dosimetric comparison of Acuros™ BV and AAPM TG-43 formalism for interstitial iridium-192 high-dose-rate brachytherapy

Yiannis Roussakis, PhD[1], Georgios Antorkas, MSc[1], Leonidas Georgiou, PhD[1], Iosif Strouthos, MD, PhD[2], Efstratios Karagiannis, MD, PhD[2], Constantinos Zamboglou, MD, PhD[2], Konstantinos Ferentinos, MD, PhD[2], Prof. Nikolaos Zamboglou, MD, PhD[2], Georgios Anagnostopoulos, PhD[1]

[1]Department of Medical Physics, German Oncology Center, University Hospital of the European University, Limassol, Cyprus, [2]Department of Radiation Oncology, German Oncology Center, University Hospital of the European University, Limassol, Cyprus

Abstract

Purpose: The aim of this study was a retrospective dosimetric comparison of iridium-192 (^{192}Ir) high-dose-rate (HDR) interstitial brachytherapy plans using model-based dose calculation algorithm (MBDCA) following TG-186 recommendations and TG-43 dosimetry protocol for breast, head-and-neck, and lung patient cohorts, with various treatment concepts and prescriptions.

Material and methods: In this study, 59 interstitial ^{192}Ir HDR brachytherapy cases treated in our center (22 breast, 22 head and neck, and 15 lung) were retrospectively selected and re-calculated with TG-43 dosimetry protocol as well as with Acuros™ BV dose calculation algorithm, with dose to medium option based on computed tomography images. Treatment planning dose volume parameter differences were determined and their significance was assessed.

Results: For the breast planning target volume (PTV), TG-43 formalism calculated higher $D_{90\%}$, $V_{95\%}$, $V_{100\%}$, and $V_{150\%}$ values than Acuros™ BV, ranging from 2.2% to 5.4% (mean differences), as it did for the head and neck cases, ranging from 2.5% to 4.7% and for the interstitial lung cases, ranging from 2.2% to 4.4%, showing statistical significance ($p < 0.001$). For the skin $D_{0.1cm3}$, $D_{0.2cm3}$, and D_{1cm3}, the values were overestimated by TG-43, with a mean absolute differences of 1.4, 1.8, and 2.0 Gy, respectively for the breast, and 1.0 Gy for all DVH statistics for the head and neck cases compared with Acuros™ BV ($p < 0.001$). Ipsilateral lung V_{5Gy} was also higher in TG-43-calculated plans, with a mean difference of 1.0% and 1.1% in the breast and lung implants, respectively. For the chest wall TG-43, the respective overestimation in $D_{0.1cm3}$ and D_{1cm3} was 0.8 and 0.8 Gy for the breast, and 0.4 and 0.3 Gy for the interstitial lung cases, respectively.

Conclusions: The TG-43 algorithm significantly overestimates the dose to PTVs and surrounding organs at risk (OARs) for breast, head and neck, and lung interstitial implants. TG-43 overestimation is in accordance with previous findings for breast and head and neck. To our knowledge, this is also exhibited for Acuros™ BV for the first time in interstitial lung HDR brachytherapy.

J Contemp Brachytherapy 2024; 16, 3: 211–218
DOI: https://doi.org/10.5114/jcb.2024.140893

Key words: HDR brachytherapy, Acuros™ BV, TG-43, heterogeneity correction, bounded anatomy.

Purpose

In contrast to the AAPM TG-43 [1-3] dosimetry protocol that is currently considered the international brachytherapy dosimetry standard, the commercially available model-based dose calculation algorithms (MBDCA) [4-6] for brachytherapy account for the effect of heterogeneities, contoured catheter material and shape as well as the limited scatter conditions in bounded patient anatomy for dose calculation. Their characteristics, the rationale of transitioning to MBDCA, and their potential for brachytherapy dosimetry have been presented by several authors [7-10]. Previous retrospective dosimetry comparison studies for clinical plans have focused on the dosimetric differences within high-dose-rate (HDR) mainly for the breast [10-14], gynecological [12, 15-18], and to a lesser extent, for head and neck [19] interstitial brachytherapy cases. The purpose of this work was to compare the dosimetry of TG-43 protocol with the grid-based Boltzmann solver (GBBS) algorithm, not only for clinical breast interstitial brachytherapy plans, but also to expand the comparison for clinical head and neck

Address for correspondence: Roussakis Yiannis, PhD, Department of Medical Physics, German Oncology Center, 1 Nikis Avenue, 4108, Agios Athanasios, Limassol, Cyprus, phone: +357-25208028, ✉ e-mail: Yiannis.Roussakis@goc.com.cy

Received: 16.01.2024
Accepted: 02.05.2024
Published: 28.06.2024

and lung iridium-192 (^{192}Ir) interstitial implants. To our knowledge, this work presented the first results of interstitial lung brachytherapy dosimetric comparisons for the Acuros^{TM} BV algorithm. Furthermore, various clinical scenarios were included for each anatomical site to allow for generalization of the results. Cases with both plastic and metallic needles, definitive and palliative schemes, and a range of prescriptions were included. This retrospective comparison was performed between the TG-43 and Acuros^{TM} BV algorithms [5] found in the BrachyVision^{TM} treatment planning system (Varian Medical Systems Inc., CA, USA). Differences of plan quality indices were computed for multi-catheter HDR brachytherapy implants in the breast, head and neck, and lung cases, where the proximity of treated clinical target volumes to bounded and/or heterogeneous anatomies raises dosimetric accuracy concerns, and the significance of dosimetric deviations was analyzed.

Material and methods

Patient cohort

Fifty-nine patients who received CT-guided interstitial multi-catheter HDR brachytherapy in our institution between 2018 and 2022 were retrospectively selected. Twenty-two patients received treatment for tumors in the breast region, twenty-two patients received treatment for tumors in the head and neck (H&N) region, while fifteen patients received treatment for the lung tumors.

Implant technique

Breast cases were implanted under sedation, and guide needles were inserted using CT-guided free-hand implantation technique. Guide needles were replaced by flexible plastic catheters (6F OncoSmart, Elekta AB), which were secured in place with radio-opaque buttons. The number of catheters ranged from 5 to 19 (median, 11; mean, 12).

Head and neck cases were implanted with CT guidance under general anesthesia. The number of catheters ranged from 1 to 12 (median, 8; mean, 7.2), while flexible plastic catheters were employed in 16 cases and stainless-steel needles (Trocar needles, Elekta AB) in 6 patients.

Lung cases were implanted with CT guidance under sedation. One (n = 13) or two (n = 2) needles were inserted for each implant, while plastic needles (ProGuide sharp, Elekta AB) were employed in 9 cases and stainless-steel needles in 6 patients. When plastic needles were used, a CT marker was inserted immediately before the final planning CT scan for better visualization of catheter paths and distal position on CT images. For treatment planning purposes, the CT marker was contoured and set to Hounsfield unit (HU) number equal to 350 (i.e., the average HU number observed within plastic catheters without CT marker), in order to represent the treatment delivery reality, where CT markers inside interstitial needles were not present.

Treatment planning

Treatment plans for all cases were optimized and calculated on CT scans obtained from General Electric Optima CT580 RT CT scanner. Most breast cases represented accelerated partial breast irradiation (APBI) with curative intends. These patients were prescribed either 32 Gy in 8 fractions or 34 Gy in 10 fractions [20-22]. In palliative breast setting, prescriptions ranged from 8 to 30 Gy in 1 to 6 fractions. Head and neck cases were treatments of palliative setting (10 lymph node metastatic cases, 3 buccal cancer cases, 2 parotid cancer cases, 2 nasal cavity cancer cases, 1 oropharyngeal, 1 base of tongue, 1 mandible, 1 maxilla, and 1 malignant peripheral nerve sheath neck tumor case), with prescriptions ranging from 24 to 30 Gy in 3 to 10 fractions [23]. Lung cases were palliative and/or re-irradiation treatments, with prescriptions ranging from 8 to 25 Gy per implant [24].

In APBI cases, planning target volume (PTV) represented a minimum of 2 cm margin around the tumor area as defined by surgical clips [20-22]. For palliative cases, gross tumor volume (GTV) also represented PTV, with no additional expansion.

All relevant organs at risk (OARs) in the vicinity of PTVs were contoured to assist treatment planning and plan evaluation. Figure 1 shows representative example cases from each anatomical site, including the respective contours generated for each case. A sub-set of those contours, for which dosimetric differences between the two algorithms due to the presence of tissue heterogeneities and/or bounded patient anatomy would be expected, were included in comparative analysis. These OARs were the skin, ipsilateral lung, and chest wall. The skin contour was defined as a 2 mm thick rind inside the external patient contour.

Treatment plans for each case were initially generated using the TG-43 algorithm, starting with inverse optimization and finalizing the plan with graphical optimization. The optimization process aimed at achieving plan objectives and constraints for each anatomical site, as proposed in respective recommendations and clinical trials [20-24]. Following finalization of the treatment plan, review, and approval by a radiation oncologist, each was retrospectively re-calculated without re-optimization using the Acuros^{TM} BV algorithm with exactly the same plans parameters (source strength, catheter reconstruction points and position, dwell positions inside each catheter, and dwell times).

For the Acuros^{TM} BV dose calculation, HU values derived from the CT scan were converted into material mass density based on HU to mass density calibration curve of the CT scanner. Iridium-192 GammaMed HDR plus source was utilized, and dose calculation grid resolution of 2.5 mm for both algorithms was selected. For Acuros^{TM} BV, dose to medium option was used.

DVH parameter analysis

Several dose volume histogram (DVH) parameters were selected for analysis, based on treatment plan objectives and constraints found in studies investigating differences in dose calculations algorithms as well as international recommendations and publications [11-24] for each treatment site. For the PTV, the dose to 90% of the volume ($D_{90\%}$), and the volume receiving 95%, 100%, and 150% of the prescribed dose ($V_{95\%}$, $V_{100\%}$, $V_{150\%}$) were applied. For the ipsilateral lung, the percentage volume

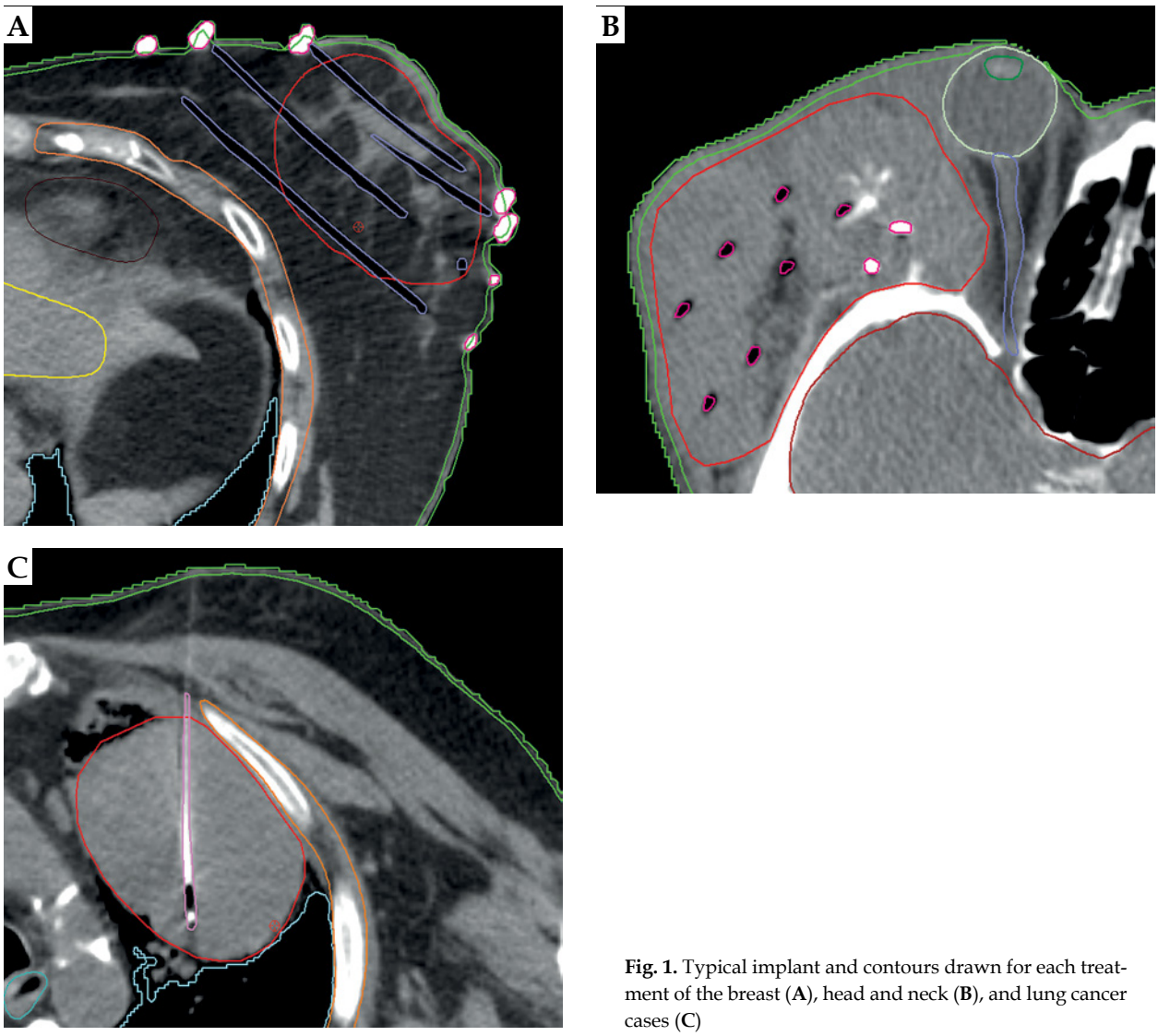

Fig. 1. Typical implant and contours drawn for each treatment of the breast (**A**), head and neck (**B**), and lung cancer cases (**C**)

receiving at least 5 Gy (V_{5Gy}). For the skin the minimum dose received by the hottest section of the contour with volume of 0.1, 0.2, and 1 cubic centimeter ($D_{0.1cm3}$, $D_{0.2cm3}$, and D_{1cm3}) were calculated, while for the chest wall, $D_{0.1cm3}$ and D_{1cm3} were considered for both the TG-43 dosimetry formalism and for Acuros™ BV.

All DVH data were generated in BrachyVision™, exported as text files and analyzed in Matlab® (MathWorks, Massachusetts, USA), where parameters for each patient and each plan were extracted. Data for each parameter were then exported into a spreadsheet. Non-parametric Wilcoxon paired test was conducted on each dataset to expose statistical significance differences using R (www.r-project.org). Statistical significance was considered with $p < 0.01$.

Results

Planning target volume

Dose volume histogram (DVH) parameter analysis results for the PTV revealed statistically significant differences ($p < 0.001$) between the dose calculated using the Acuros™ BV compared with the TG-43 algorithm. Specifically, as summarized in Table 1, Acuros™ BV calculated lower doses for all DVH parameters analyzed ($D_{90\%}$, $V_{95\%}$, $V_{100\%}$, and $V_{150\%}$). For the breast, the mean percentage differences from TG-43 ((Acuros™ BV – TG-43)/TG-43) ranged from –2.2% to –5.4%, for the head and neck cases, they ranged from –2.5% to –4.7%, while for the lung cases, the values ranged from –2.2% to –4.4%, with all of the mean percentage differences showing statistical significance ($p < 0.001$). Figure 2 shows a box and whisker plot of the PTV parameters analyzed, where is evident that TG-43 clearly overestimated the dose coverage of the PTV for each anatomical site, since it did not account for the missing scatter photon dose component in the vicinity of the PTV to the lung and/or PTV to patient body boundaries. The highest $D_{90\%}$ mean percentage difference was evident in the lung PTV, where the PTVs were anatomically mostly surrounded by air-inflated lung tissue. For the breast cases, the maximum percentage dose difference of Acuros™ BV from TG-43 for $D_{90\%}$ was equal

Table 1. Analysis of dose to planning target volume (PTV) showing median and mean percentage difference of dose calculated with Acuros™ BV from that calculated using TG-43 algorithms ((Acuros™ BV – TG-43)/TG-43), with 1st and 3rd quartiles (Q1-Q3), standard error, and *p*-value calculated using Wilcoxon paired test

DVH parameter	Breast cases			Head & neck cases			Lung cases		
	Median (Q1 to Q3)	Mean ±SE	*p*-value	Median (Q1 to Q3)	Mean ±SE	*p*-value	Median (Q1 to Q3)	Mean ±SE	*p*-value
PTV $D_{90\%}$ (%)	–3.7 (-4.8 to –2.5)	–4.2 ±0.5	< 0.001	–4.3 (–5.7 to –3.2)	–4.0 ±0.4	< 0.001	–4.0 (–4.4 to –3.6)	–4.5 ±0.5	< 0.001
PTV $V_{95\%}$ (%)	–1.8 (–3.3 to –1.1)	–2.0 ±0.3	< 0.001	–2.7 (–3.3 to –1.9)	–2.2 ±0.2	< 0.001	–1.8 (–2.3 to –1.7)	–2.1 ±0.4	< 0.001
PTV $V_{100\%}$ (%)	–2.3 (–3.7 to –1.4)	–2.7 ±0.4	< 0.001	–3.0 (–3.7 to –2.2)	–2.5 ±0.2	< 0.001	–2.1 (–2.6 to –1.8)	–2.3 ±0.4	< 0.001
PTV $V_{150\%}$ (%)	–4.8 (–7.3 to –2.9)	–2.9 ±0.3	< 0.001	–4.4 (–5.9 to –3.6)	–2.6 ±0.2	< 0.001	–3.4 (–4.0 to –2.8)	–2.3 ±0.3	< 0.001

DVH – dose volume histogram, PTV – planning target volume, $V_{x\%}$ – volume receiving x% of the prescribed dose, $D_{x\%}$ – dose received by x% of the volume (as a percentage to the prescribed dose), Q1 – 1st quartile, Q3 – 3rd quartile, SE – standard error

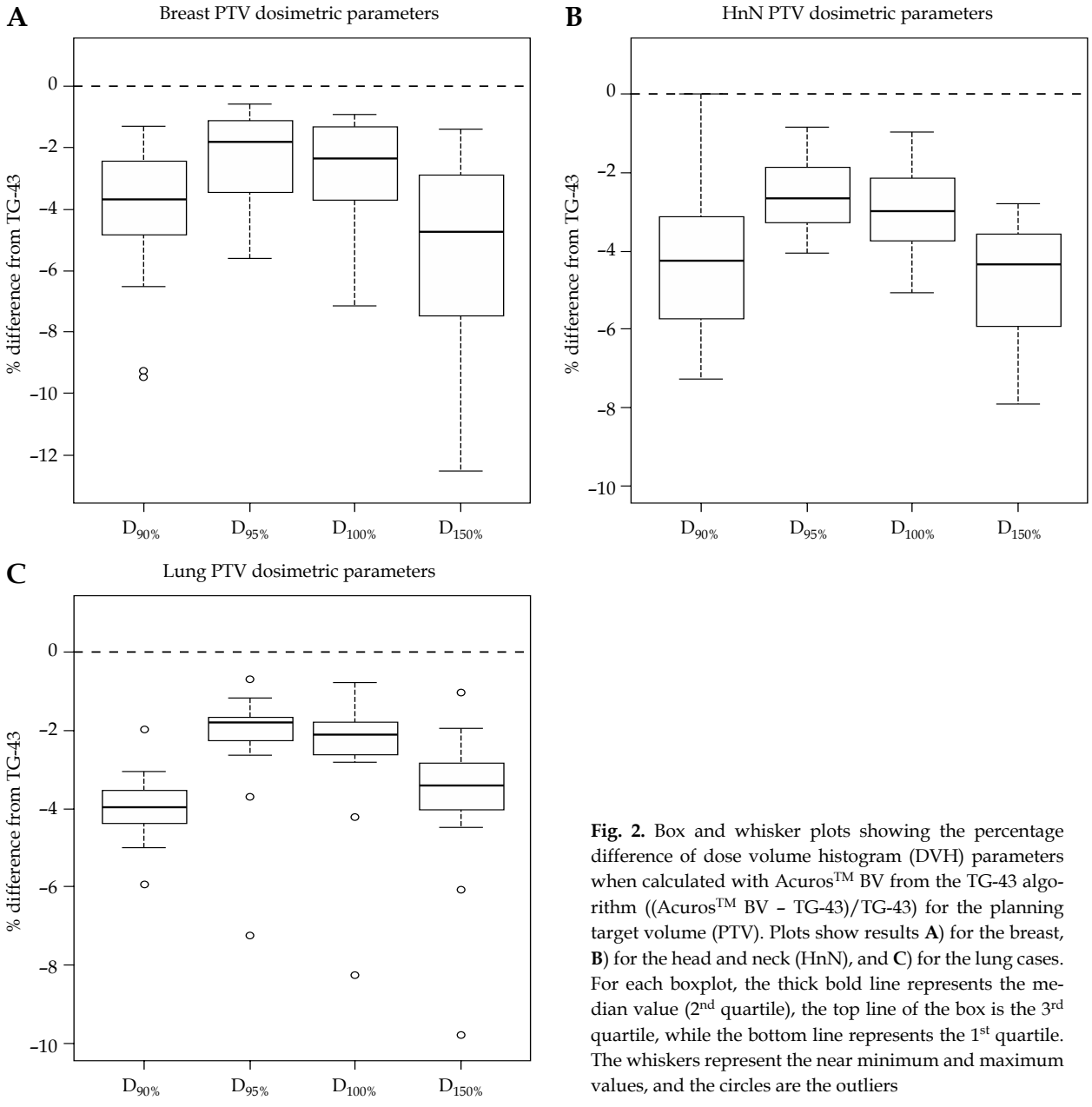

Fig. 2. Box and whisker plots showing the percentage difference of dose volume histogram (DVH) parameters when calculated with Acuros™ BV from the TG-43 algorithm ((Acuros™ BV – TG-43)/TG-43) for the planning target volume (PTV). Plots show results **A**) for the breast, **B**) for the head and neck (HnN), and **C**) for the lung cases. For each boxplot, the thick bold line represents the median value (2nd quartile), the top line of the box is the 3rd quartile, while the bottom line represents the 1st quartile. The whiskers represent the near minimum and maximum values, and the circles are the outliers

to –10.7%, for $V_{95\%}$, it was –5.5%, for $V_{100\%}$, –6.8%, and for $V_{150\%}$, it was –5.9%, while for the head and neck cases, the maximum percentage dose difference were equal to –7.5%, –3.7%, –4.5%, and –4.7%, respectively. For the lung cases, the maximum dose percentage differences were equal to –11.3% for $D_{90\%}$, –6.8% for $V_{95\%}$, –7.6% for $V_{100\%}$, and –5.3% for $V_{150\%}$. The higher dose overestimation by the TG-43 formalism for $D_{90\%}$ and $V_{100\%}$ was more pronounced for interstitial lung cases, where PTVs were almost completely surrounded by air-inflated lung tissue, and not in anatomical regions close to a homogeneous structure (i.e., the liver).

Organs at risk

The results of DVH parameter analysis for organs at risk also revealed important differences in certain stages of the dose calculated by the two algorithms. Table 2 summarizes the results of the absolute dose difference for the skin, chest wall, and ipsilateral lung, which were common in most of the cases, revealing statistically significant differences. Acuros™ BV calculated lower dose for all skin DVH parameters analyzed ($D_{0.1cm3}$, $D_{0.2cm3}$, and D_{1cm3}). For the breast implants, the mean absolute differences were –1.4, –1.8, and –2.0 Gy (Acuros™ BV – TG-43), respectively, while for the head and neck region, the mean absolute differences were –1.0 for all DVH statistics, showing statistical significance ($p < 0.01$). The ipsilateral lung V_{5Gy} was also calculated lower by Acuros™ BV, with the mean difference of –1% for the breast cases ($p < 0.01$) and –2% for the lung region ($p < 0.001$). For the chest wall, the absolute difference of median dose values for $D_{0.1cm3}$ and D_{1cm3} was 0.6 and 0.5 Gy (ranging from 0.1 to 2.2 Gy) for the breast implants, and 0.6 and 0.7 Gy (ranging from 0.1 to 0.8 Gy) for the interstitial lung implants, respectively, with TG-43 calculating higher dose values than Acuros™ BV, demonstrating statistical significance ($p < 0.001$). The maximum absolute dose overestimation of the TG-43 formalism in comparison with Acuros™ BV was equal to 2.2 and 2.1 Gy for $D_{0.1cm3}$ and D_{1cm3}, and 0.6 and 0.8 Gy for $D_{0.1cm3}$ and D_{1cm3} for the lung implant, respectively. Figure 3 shows a box and whisker plot of the skin dose parameters analyzed, where it is evident that TG-43 clearly overestimated the dose received by the skin for both the breast and head and neck cases due to the inability of TG-43 to account for bounded patient geometry. For the breast, the maximum absolute dose overestimation by TG-43 for the skin $D_{0.2cm3}$ was equal to 10.9 Gy, but this was because the PTV was extended inside the skin contour due to skin infiltration by the tumor, and because of the catheter vicinity (< 1 cm), which resulted in the presence of high-dose gradients.

Discussion

Since the Acuros™ BV algorithm is known for its ability to account for heterogeneities and bounded patient anatomy by providing dosimetric accuracy comparable with Monte Carlo (MC) dose calculations [10], it was employed in the current study to retrospectively calculate 22 breast, 22 head and neck, and 15 lung cases, and to compare the dosimetric results with the TG-43 dose formalism, as it has been presented previously by several groups and summarized in a recent review article [25]. A notable difference of the current study is the analysis of a wide and heterogeneous group of cases, with varying anatomical localization of the tumor, total prescribed dose, fractionation, and type of implant material employed (i.e., plastic or metal needles). This heterogeneity was chosen to demonstrate the expected range of differences across many possible clinical scenarios.

For the breast PTV, all dosimetric results showed a statistically significant dose overestimation by the TG-43 formalism in comparison with Acuros™ BV, which agrees with previous findings of 4% reported by Sinnatamby *et al*. [13]. This is also evident for all head and

Table 2. Analysis of dose to selected organs at risk showing median and mean difference of dose calculated with Acuros™ BV from that calculated using TG-43 algorithms, with 1st and 3rd quartiles (Q1-Q3), standard error, and *p*-value calculated using Wilcoxon paired test

DVH parameter	Breast cases			Head & neck cases			Lung cases		
	Median (Q1 to Q3)	Mean ±SE	*p*-value	Median (Q1 to Q3)	Mean ±SE	*p*-value	Median (Q1 to Q3)	Mean ±SE	*p*-value
Skin $D_{0.1cm3}$ (Gy)	–1.0 (–2.2 to –0.4)	–2.0 ±0.8	< 0.001	–0.9 (–1.5 to –0.4)	–1.0 ±0.2	< 0.001	N.A.	N.A.	N.A.
Skin $D_{0.2cm3}$ (Gy)	–1.0 (–2.2 to –0.4)	–1.7 ±0.5	< 0.001	–0.9 (–1.5 to –0.4)	–1.0 ±0.2	< 0.001	N.A.	N.A.	N.A.
Skin D_{1cm3} (Gy)	–1.2 (–2.2 to –0.4)	–1.4 ±0.2	< 0.001	–0.9 (–1.6 to –0.3)	–1.0 ±0.2	< 0.001	N.A.	N.A.	N.A.
Ipsilateral lung V_{5Gy} (%)	–0.4 (–0.7 to 0.0)	–1.0 ±0.5	< 0.010	N.A.	N.A.	N.A.	–0.6 (–1.0 to –0.2)	–1.1 ±0.4	< 0.010
Chest wall $D_{0.1cm3}$ (Gy)	–0.5 (–1.0 to –0.4)	–0.8 ±0.1	< 0.001	N.A.	N.A.	< 0.001	–0.4 (–0.5 to –0.3)	–0.4 ±0.1	< 0.001
Chest wall D_{1cm3} (Gy)	–0.5 (–1.0 to –0.4)	–0.8 ±0.2	< 0.001	N.A.	N.A.	< 0.001	–0.4 (–0.5 to –0.1)	–0.3 ±0.1	< 0.001

DVH – dose volume histogram, D_{xcm3} – dose to the hottest x cubic centimeters volume; V_{xGy} – volume receiving xGy; Q1 – 1st quartile, Q3 – 3rd quartile, SE – standard error

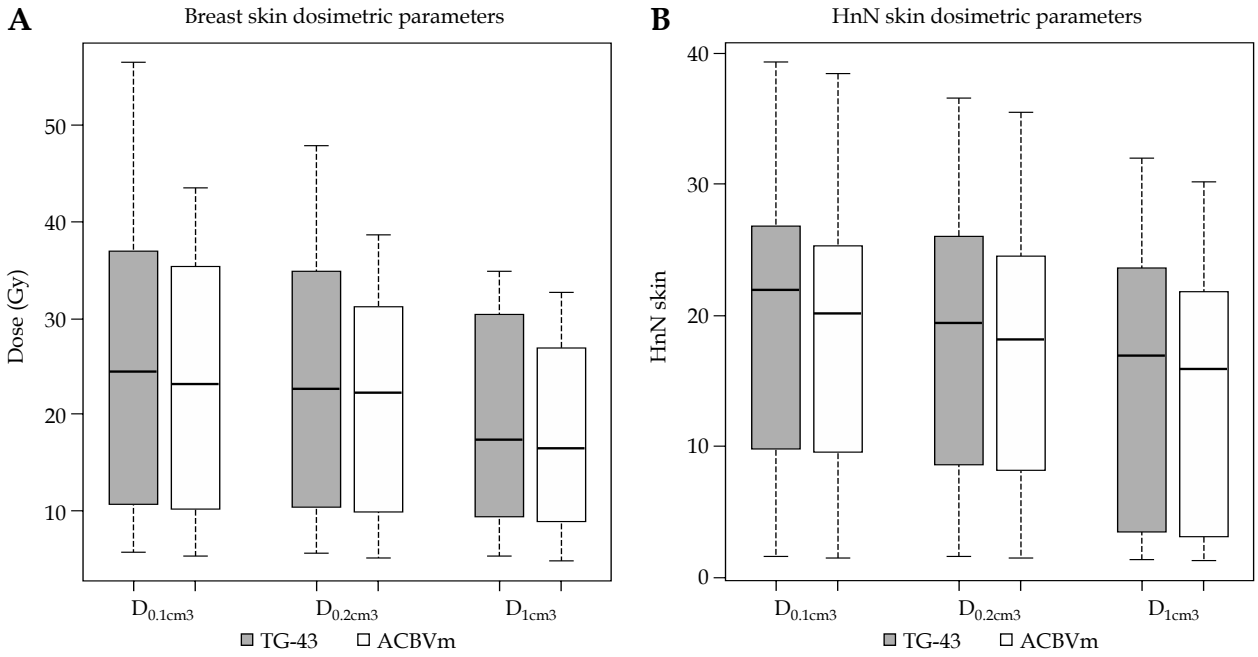

Fig. 3. Box and whisker plots showing the absolute differences of dose volume histogram (DVH) parameters when calculated with Acuros^{TM} BV from the TG-43 algorithm for the skin in treatments of the breast (**A**), and head and neck (HnN) region (**B**). For each boxplot, the thick bold line represents the median value (2nd quartile), the top line of the box is the 3rd quartile, while the bottom line represents the 1st quartile. The whiskers represent the near minimum and maximum values, and the circles are the outliers

neck cases in our study, and in accordance with findings of Siebert *et al*. [19] who reported $V_{100\%}$ and $D_{90\%}$ median dose overestimations by TG-43 with 3%. TG-43 overestimated $V_{150\%}$ more than it did for $V_{100\%}$. For example, in breast implants, $V_{150\%}$ percentage difference between the two algorithms was 5.4%, and for $V_{100\%}$, it was 2.9%, i.e., 86% higher. A similar pattern was seen for head and neck implants, where $V_{150\%}$ percentage difference between the algorithms was 4.7%, and for $V_{100\%}$, it was 2.9%, i.e., 62% higher. The TG-43 formalism calculated median $V_{150\%}/V_{100\%}$ ratio, and was higher by 3.7% for the breast and by 2.7% for the head and neck implants, in comparison with Acuros^{TM} BV. Therefore, Acuros^{TM} BV calculated plans generally resulted in more homogeneous dose distributions in our study. This comes in line with an increase of dose homogeneity index of 8% in Acuros^{TM} BV when compared with TG-43, as reported previously by Sinnatamby *et al*. [13] for the breast. It should be noted that, as the user focuses on the dosimetric analysis with higher percentage dose values (> 200%), dose volume calculations should be considered with caution; because of steep dose gradient, uncertainties of more than 10% may arise [26].

For the interstitial lung cases, all dose coverage indices were statistically higher for the TG-43 protocol than that calculated by Acuros^{TM} BV as well as $V_{150\%}$. The dose coverage reduction calculated with Acuros^{TM} BV was contrary to previous findings reported by O'Connel *et al*. [27] using the Elekta MBDCA algorithm, where a dose increase of 7% for $D_{90\%}$ and 3% for $V_{100\%}$ was reported. To our knowledge, there is no study that investigated Acuros^{TM} BV dose difference compared with TG-43 for lung implants. The higher discrepancies for $D_{90\%}$ and $V_{100\%}$ were found for cases, in which the PTVs were surrounded by air-inflated lung tissue.

The skin mean dose indices differences in the current work were significantly higher for TG-43 than that calculated with Acuros^{TM} BV. The maximum skin dose differences were observed in the vicinity of the catheters, when the PTVs included the skin, in the case where the tumor has infiltrated the skin, and the PTV was adjacent or overlapping the skin contour. The skin $D_{0.1cm3}$ and D_{1cm3} overestimation by TG-43 in the present study was lower than the one reported by Hofbauer *et al*. [12] who reported values equal to 5.7% and 6.7%, respectively. This may be attributed to the position of the implant in relation to the skin and to the method for skin delineation used by Hofbauer *et al*. [12]. Generally, for small structure volumes following recommendations by Kirisits *et al*. [26], large differences should be handled with care, since uncertainties in DVH dose calculation are higher for smaller volumes than for larger ones.

In the breast implant, the chest wall median dose indices were also statistically significantly higher for TG-43 compared with Acuros^{TM} BV, as reported previously by Hofbauer *et al*. study [12]. Although the median TG-43 $D_{0.1cm3}$ and D_{1cm3} for all breast cases were 0.6 and 0.5 Gy higher than Acuros^{TM} BV respective values, for the case of deeply located breast implants in the vicinity of the chest wall and ipsilateral lung, the TG-43 dose discrepancy from Acuros^{TM} BV became more profound. This finding has been reported by Zourari *et al*. [10], and also observed in the current study, where a 2.2 and 2.1 Gy for $D_{0.1cm3}$ and D_{1cm3} TG-43 overestimations as compared with Acuros^{TM} BV for a deep-seated breast implant were reported. This is attributed to the inability of TG-43 to account for

the lack of backscatter due to the presence of ipsilateral lung in a region relatively close to the border of CTV. For the interstitial lung implants, the maximum absolute chest wall dose overestimations of 0.6 and 0.8 Gy by TG-43 compared with Acuros™ BV was less pronounced in comparison with the breast implants. This may be attributed to the fact that in the case where the solid mass lung tumor lies in the close vicinity of the chest wall, this organ at risk is encompassed on one side by the solid tumor, and on the other side by the adipose or breast tissue; thus, leading to a situation of higher scatter conditions compared with a situation of the breast implants, where on one side of the chest wall, the presence of air-inflated lung leads to a lower backscatter conditions, causing TG-43 to deviate from Acuros™ BV more profoundly than in the case of the chest wall lying in the vicinity of the lung tumor implant.

The lung V_{5Gy} was statistically significantly higher when calculated with TG-43 compared with Acuros™ BV by 1% for both the breast and lung cases. Since the 5 Gy isodose line for our breast implants was lower than 20% of the prescribed isodose, this overestimation was due to the inability of TG-43 to account for the lack of scatter photon dose component due to the presence of air-inflated lung in an area further away from the implanted catheters. In this area, the scattered photon dose component plays the predominant role, which is in line with findings of Pantelis *et al*. [28] for isodoses of less than 60% of the prescribed dose.

Conclusions

The undisputed benefit of Acuros™ BV in dosimetric calculation accuracy lies in its ability to account for the tissue as well as the brachytherapy catheter material (i.e., stainless steel or titanium needles) heterogeneities as well as the bounded anatomical geometry of the patient contour around the PTV and OARs, which may exhibit totally different tissue characteristics (bone and/or air) from the ones considered by the TG-43 formalism. In our work, Acuros™ BV calculates significantly lower doses to PTVs for the breast, head and neck, and lung implants as well as for the surrounding OARs. In specific cases, this might lead to a dose important coverage reduction not carefully accounted for, if only the TG-43 formalism is considered for dose calculation and dose reporting. As stated in a study by Papagiannis *et al*. [8], the benefit of Acuros™ BV as a MBDCA lies in the amount of reduction in the response to clinical trial populations through the individualization of patient dosimetry. In order to move to a fully model-based optimization in clinical practice, clinical trials for confirmation and/or re-evaluation of the current dosimetric objectives and constraints are needed, since these established from clinical trials and TG-43-based algorithms were solely applied.

Acknowledgements

The authors would like to thank Dr. Stavroula Giannouli, Mrs. Rebecca Park, and Dr. Georg Schwickert from Varian Medical Systems Inc., a Siemens Healthineers Company, for BrachyVision TM software technical assistance and their valuable recommendations.

Funding

This work was partially funded by Varian Medical Systems Inc., a Siemens Healthineers Company.

Disclosures

Approval of the Bioethics Committee was not required.

The authors report no conflict of interest.

References

1. Nath R, Anderson LL, Luxton G et al. Dosimetry of interstitial brachytherapy sources: recommendations of the AAPM Radiation Therapy Committee Task Group No. 43. American Association of Physicists in Medicine. *Med Phys* 1995; 22: 209-234.
2. Rivard MJ, Butler WM, DeWerd LA et al. Supplement to the 2004 update of the AAPM Task Group No. 43 Report. *Med Phys* 2007; 34: 2187-2205.
3. Rivard MJ, Coursey BM, DeWerd LA et al. Update of AAPM Task Group No. 43 Report: a revised AAPM protocol for brachytherapy dose calculations. *Med Phys* 2004; 31: 633-674.
4. Beaulieu L, Carlsson Tedgren A, Carrier JF et al. Report of the Task Group 186 on model-based dose calculation methods in brachytherapy beyond the TG-43 formalism: Current status and recommendations for clinical implementation. *Med Phys* 2012; 39: 6208-6236.
5. Acuros BV. Algorithm Reference Guide, Document ID B504878R01A, Revision A. 2013; 8: 1-36.
6. Van Veelen B, Ma Y, Beaulieu L. Whitepaper: ACE Advanced Collapsed cone Engine. Veenendal, the Netherlands: Elekta Corporation, 2015.
7. Enger SA, Vijande J, Rivard MJ. Model-based dose calculation algorithms for brachytherapy dosimetry. *Semin Radiat Oncol* 2019; 30: 77-86.
8. Papagiannis P, Pantelis E, Karaiskos P. Current state of the art brachytherapy treatment planning dosimetry algorithms. *Br J Radiol* 2014; 87: 20140163.
9. Sloboda RS, Morrison H, Cawston-Grant B et al. A brief look at model-based dose calculation principles, practicalities, and promise. *J Contemp Brachytherapy* 2017; 9: 79-88.
10. Zourari K, Pantelis E, Moutsatsos A et al. Dosimetric accuracy of a deterministic radiation transport based ^{192}Ir brachytherapy treatment planning system. Part III. Comparison to Monte Carlo simulation in voxelized anatomical computational models. *Med Phys* 2013; 40: 011712.
11. Howie A, Poder J, Brown R et al. Comparison of TG43 and Hounsfield Unit- based TG186 brachytherapy dose metrics in Oncentra Brachy for 100 patients receiving interstitial partial breast irradiation. *Brachytherapy* 2021; 20: 655-663.
12. Hofbauer J, Kirisits C, Resch A et al. Impact of heterogeneity corrected dose calculation using a grid-based Boltzmann solver on breast and cervix cancer brachytherapy. *J Contemp Brachytherapy* 2016; 8: 143-149.
13. Sinnatamby M, Vivekanandan N, Sathyanarayana R et al. Dosimetric comparison of Acuros™ BV with AAPM TG43 dose calculation formalism in breast interstitial high-dose-rate brachytherapy with the use of metal catheters. *J Contemp Brachytherapy* 2015; 7: 273-279.
14. Thrower SL, Shaitelman SF, Bloom E et al. Comparison of dose distributions with TG-43 and collapsed cone convolution algorithms applied to accelerated partial breast irra-

diation patient plans. *Int J Radiat Oncol Biol Phys* 2016; 95: 1520-1526.
15. Bi SY, Chen ZJ, Sun X et al. Dosimetric comparison of AcurosBV with AAPM TG43 dose calculation formalism in cervical intraductal high-dose rate brachytherapy using three different applicators. *Prec Radiat Oncol* 2022; 6: 234-242.
16. Radcliffe BA, Meltsner S, Yongbok K et al. PHSOR08 Retrospective Comparison of TG43 vs. AcurosBV model-based dose calculation algorithm (MBDCA) in cervical cancer patients treated with HDR brachytherapy boost. *Brachytherapy* 2022; 21: S27-S28.
17. Dagli A, Yurt F, Yegin G. Evaluation of BrachyDose Monte Carlo code for HDR brachytherapy: dose comparison against Acuros® BV and TG-43 algorithms. *J Radiother Pract* 2020; 19: 76-83.
18. Mikell JK, Klopp AH, Gonzalez Gonzalez MN et al. Impact of heterogeneity-based dose calculation using a deterministic grid-based Boltzmann equation solver for intracavitary brachytherapy. *Int J Radiat Oncol Biol Phys* 2012; 83: e417-e422.
19. Siebert FA, Wolf S, Kóvacs G. Head and neck ^{192}Ir HDR-brachytherapy dosimetry using a grid-based Boltzmann solver. *J Contemp Brachytherapy* 2013; 5: 232-235.
20. Strand V, Major T, Polgar C et al. ESTRO-ACROP guideline: Interstitial multi-catheter breast brachytherapy as accelerated partial breast irradiation alone or as boost – GEC-ESTRO Breast Cancer Working Group practical recommendations. *Radiother Oncol* 2018; 128: 411-420.
21. Arthur DW, Vicini FA, Kuske RR et al. Accelerated partial breast irradiation: an updated report from the American Brachytherapy Society. *Brachytherapy* 2003; 2: 124-130.
22. Strnad V, Krug D, Sedlmayer et al. DEGRO practical guidance for partial-breast irradiation. *Strahlenther Onkol* 2020; 196: 749-763.
23. Kovacs G, Martinez-Monge R, Budrukkar A et al. GEC-ESTRO ACROP recommendations for head & neck brachytherapy in squamous cell carcinomas: 1st update – Improvement by cross sectional imaging based treatment planning and stepping source technology. *Radiother Oncol* 2017; 122: 248-254.
24. Ferentinos K, Karagiannis E, Strouthos I et al. Computed tomography guided interstitial percutaneous high-dose-rate brachytherapy in the management of lung malignancies. A review of the literature. *Brachytherapy* 2021; 20: 892-899.
25. Yousif AMY, Osman AFI, Halato MA. A review of dosimetric impact implementation of dose calculation algorithms (MBDCAs) for HDR brachytherapy. *Phys Eng Sci Med* 2021; 44: 871-886.
26. Kirisits C, Siebert FA, Baltas D et al. Accuracy of volume and DVH parameters determined with different brachytherapy treatment planning systems. *Radiother Oncol* 2007; 84: 290-297.
27. O'Connell D, Chang A, Lee A et al. TH-A-TRACK 3–07: investigating the impact of model-based dose calculation on interstitial lung brachytherapy and comparison to external beam SBRT. *Med Phys* 2020; 47: e367.
28. Pantelis E, Papagiannis P, Karaiskos P et al. The effect of finite patient dimensions and tissue inhomogeneities on dosimetry planning of 192Ir HDR breast brachytherapy: a Monte Carlo dose verification study. *Int J Radiat Oncol Biol Phys* 2005; 61: 1596-1602.